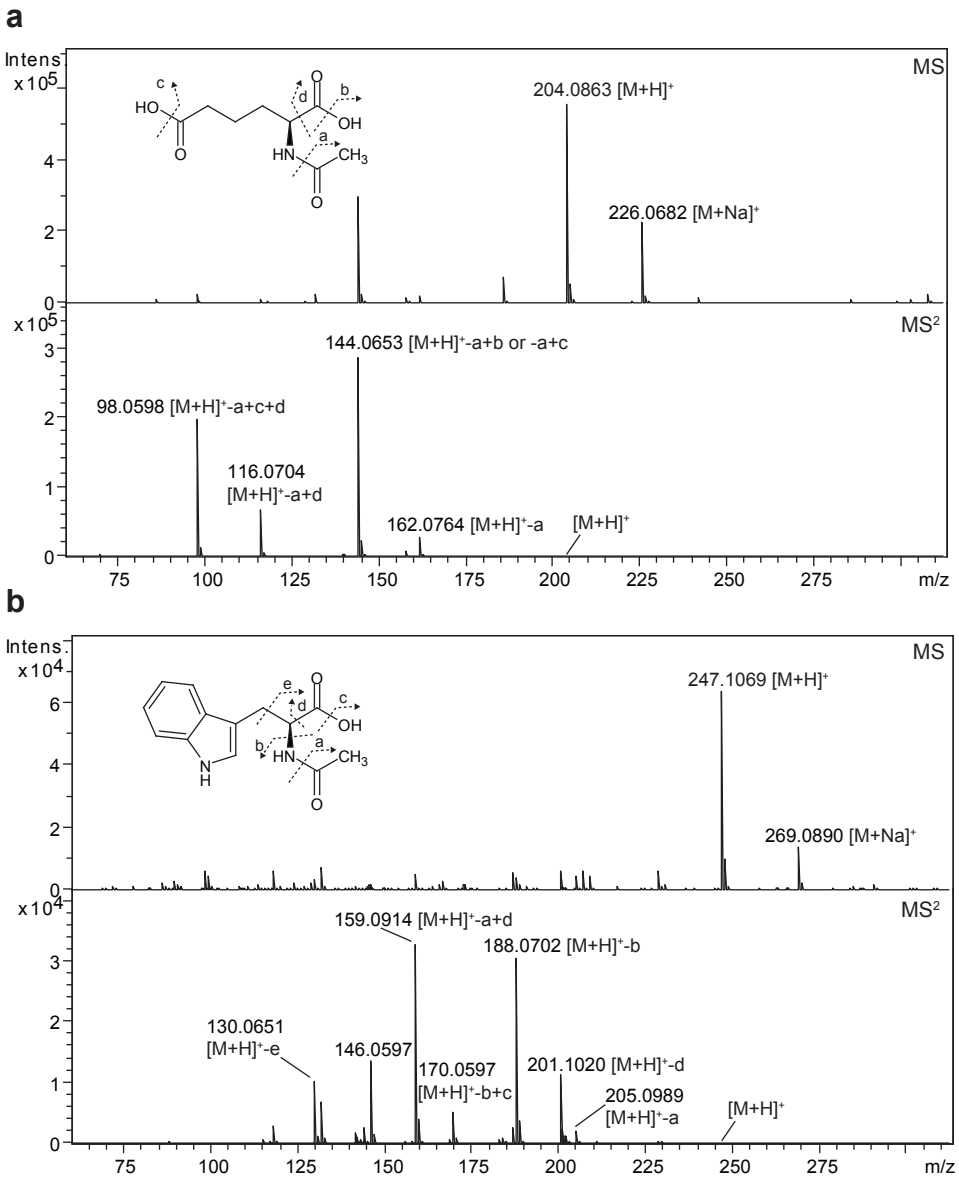

Supplementary Figure 1 | Liquid chromatography-tandem mass spectrometry (LC-MS2) identification of N-acetyl-L-aminoadipate (a) and N-acetyl-L-tryptophan (b) accumulating in senescent leaves *clh2-1* (FLAG_076H05). MS and MS^2 spectra, chemical structures and fragmentation pattern are shown. Calculated $[M+H]^+$ adducts for acetyl-aminoadiate and acetyl-tryptophan are 204.0866 m/z and 247.1077 m/z, respectively. Note that the fragmentation pattern for N-acetyl-D/L-aminoadipate and N-acetyl-D/L-tryptophan is concordant with the fragmentation pattern of L-aminoadipate, L-tryptophan and N-Acetyl-DL-tryptophan as in METLIN database (https://metlin.scripps.edu/index.php [36]) and as published previously[25].

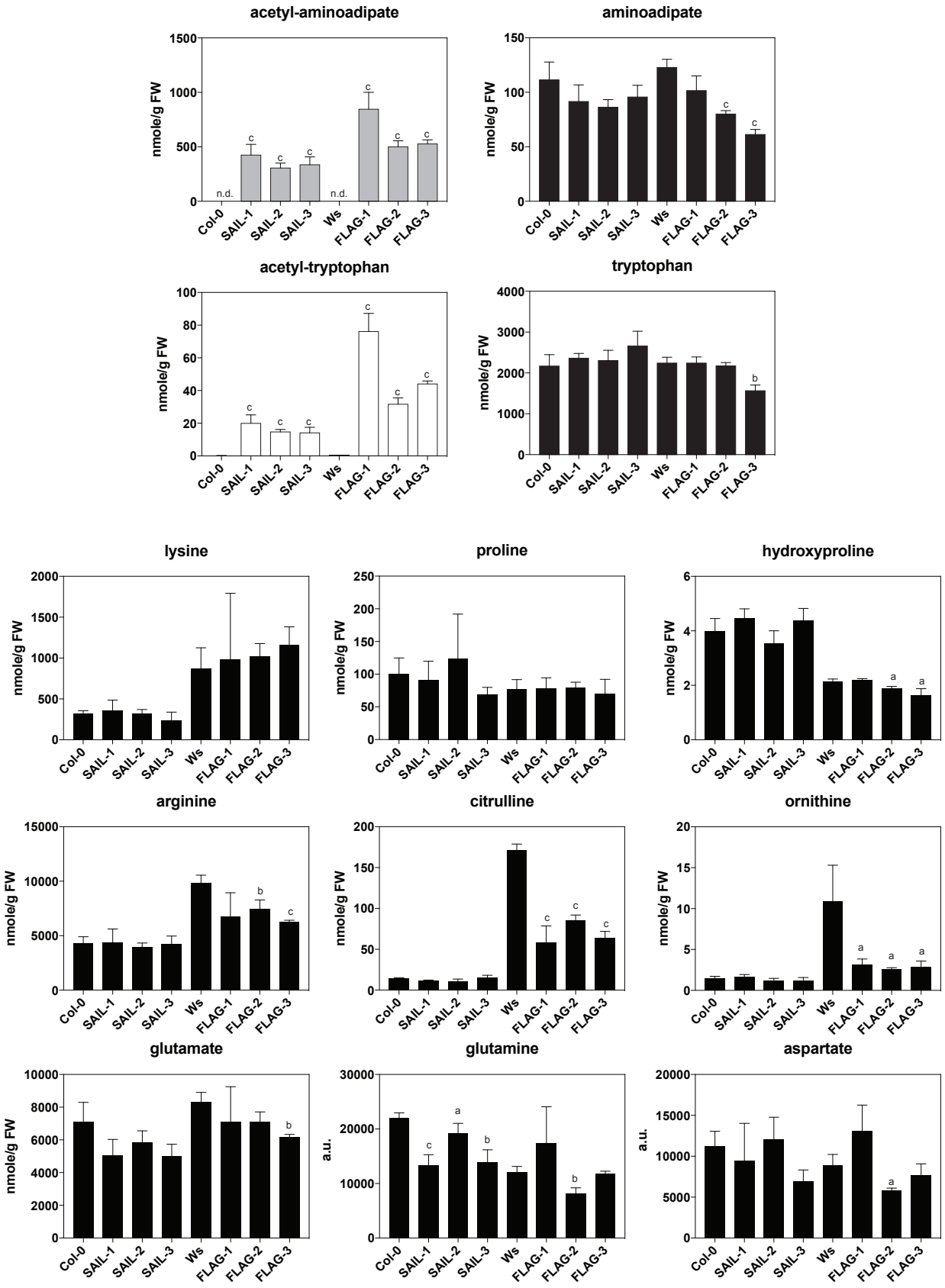

Supplementary Figure 2| *Continues on next page*

(continued)

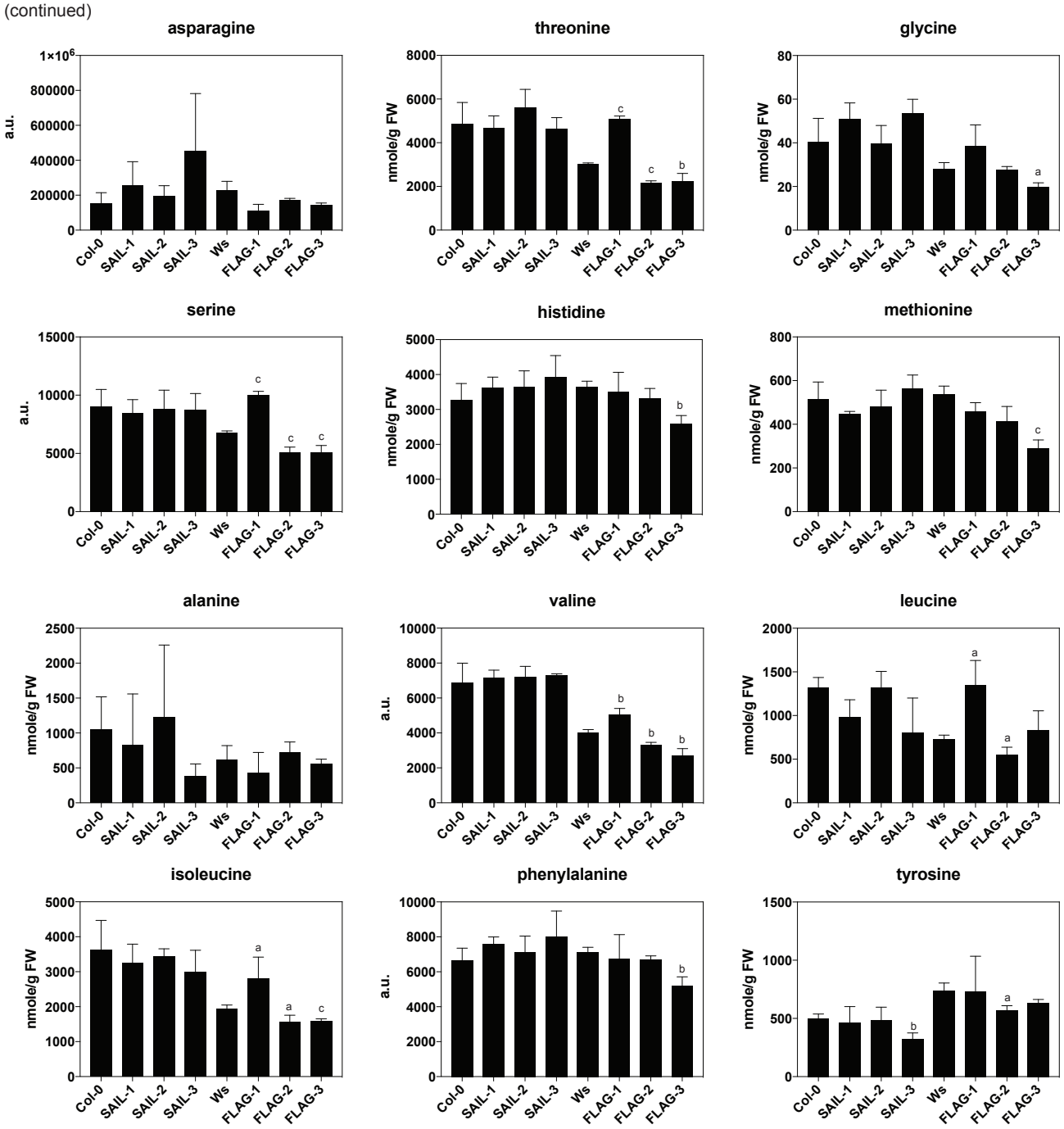

Supplementary Figure 2 | Quantification of free amino acids in senescent leaves of BAR-containing Arabidopsis. Absolute quantification of acetyl-aminoadipate, aminoadipate, acetyl-tryptophan and tryptophan, and relative or absolute quantification of 21 other free amino acids in SAIL and FLAG lines. Error bars, mean ± s.d. (n = 3 biological replicates). Significance levels were indicated based on unpaired Student t-tests with correction for multiple comparison using the Holm-Sidak method. a, p-value<0.1; b, p-value<0.05; c, p-value<0.01. Note that values for a few amino acids are shown as relative levels (a.u., arbitrary unit.) because their concentrations in some samples were more than 10-fold higher than the highest concentration of the standard.

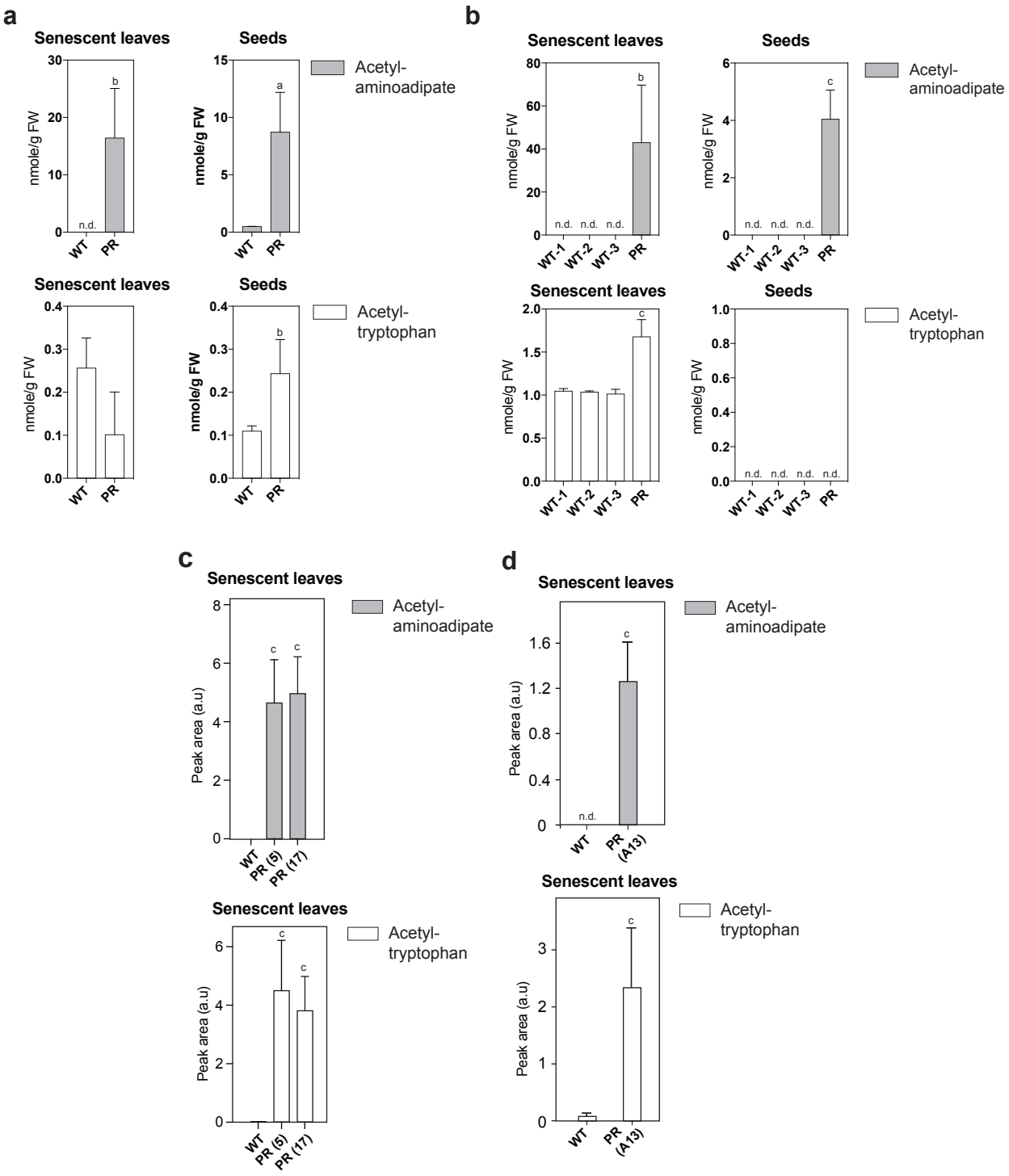

Supplementary Figure 3 | Accumulation of acetyl-aminoadipate and acetyl-tryptophan in senescent leaves and seeds of phosphinothricin-resistant (PR) *Glycine max*, *Brassica napus, Brassica juncea and Triticum aestivum*. **a,** Absolute quantification of acetyl-aminoadipate and acetyl-tryptophan in senescent leaves and seeds of phosphinothricin-resistant *Glycine max* (WT, Chiba Green wild-type; PR, Liberty Link trait A2704-12 (Bayer CropScience). **b**, Absolute quantification of acetyl-aminoadipate and acetyl-tryptophan in senescent leaves and seeds of phosphinothricin-resistant *Brassica napus* (WT-1 (control-1), NDC-E12131; WT-2 (control-2), NDC-E13285; WT-3 (control-3), NDC-E12027; PR, Liberty Link trait L252, Bayer CropScience). Note that isogenic lines controls could not be obtained for *Glycine max* and *Brassica napus* PR lines. **c**, Relative quantification of acetyl-aminoadipate and acetyl-tryptophan in senescent leaves of phosphinothricin-resistant *Brassica juncea* (WT, wild-type isogenic line; PR (5 and 17), phosphinothricin-resistant lines[31]). **d**, Relative quantification of acetyl-aminoadipate and acetyl-tryptophan in senescent leaves of phosphinothricin-resistant *Triticum aestivum* (WT, wild-type isogenic line; PR (A13), phosphinothricin-resistant line[32]). Error bars, mean ± s.d. (n = 3 biological replicates). Significance levels were indicated based on unpaired Student t-tests. a, p-value<0.1; b, p-value<0.05; c, p-value<0.01. For *Brassica napus*, the highest p-values obtained by comparison of each wild-type with the phosphinothricin-resistant line are indicated.

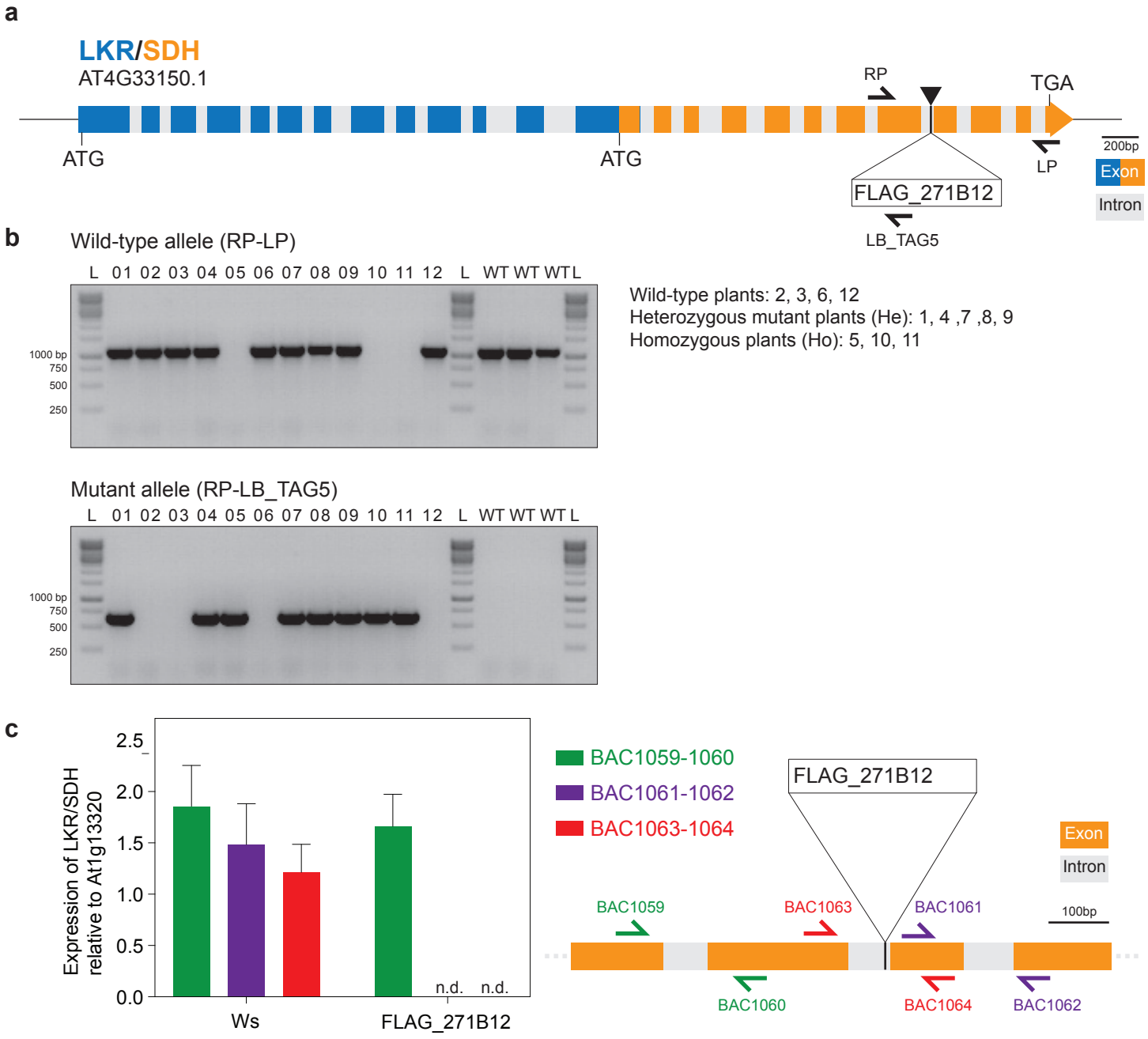

Supplementary Figure 4 | Genotyping of FLAG_*lkrsdh* and analysis of LKR/SDH expression. a, Gene structure of Arabidopsis LKR/SDH (AT4G33150.1). LKR and SDH exons are depicted in blue and orange, respectively. The T-DNA insertion site and genotyping primers for FLAG_*lkrsdh* (FLAG_271B12) are indicated. ATG and TGA depict start and stop codons. **b**, Genotyping by PCR of the segregating population (12 plants) of FLAG_*lkrsdh* used for the experiment presented in Figure 2. The genotype of each individual is indicated on the right. WT, Wild-type Wassilewskija control. **c**, Analysis of gene expression in homozygous mutant FLAG_*lkrsdh* by quantitative real-time PCR. The expression of LKR/SDH was normalized to the reference gene At1g13320[30]. The positions of the three primer sets used for this analysis are depicted on the right. n.d., not detected.

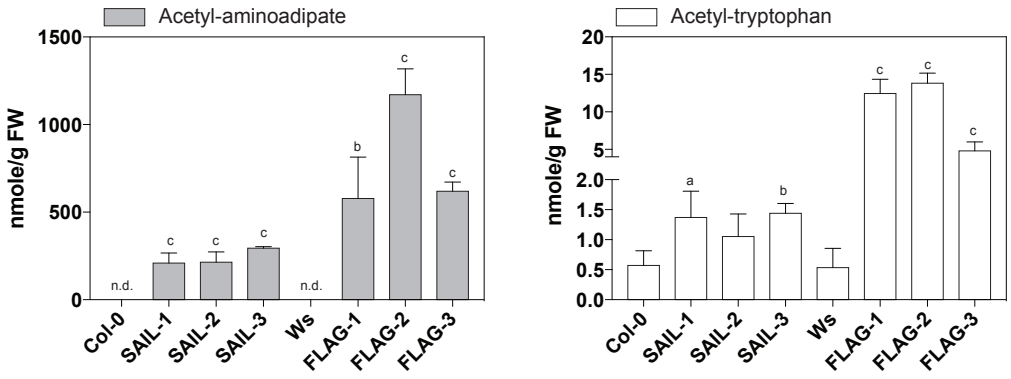

Supplementary Figure 5 | Absolute quantification of acetyl-aminoadipate and acetyl-tryptophan in seeds of BAR-containing Arabidopsis. Error bars, mean ± s.d. (n = 3 biological replicates). Significance levels were indicated based on unpaired Student t-tests with correction for multiple comparison using the Holm-Sidak method. a, p-value<0.1; b, p-value<0.05; c, p-value<0.01.

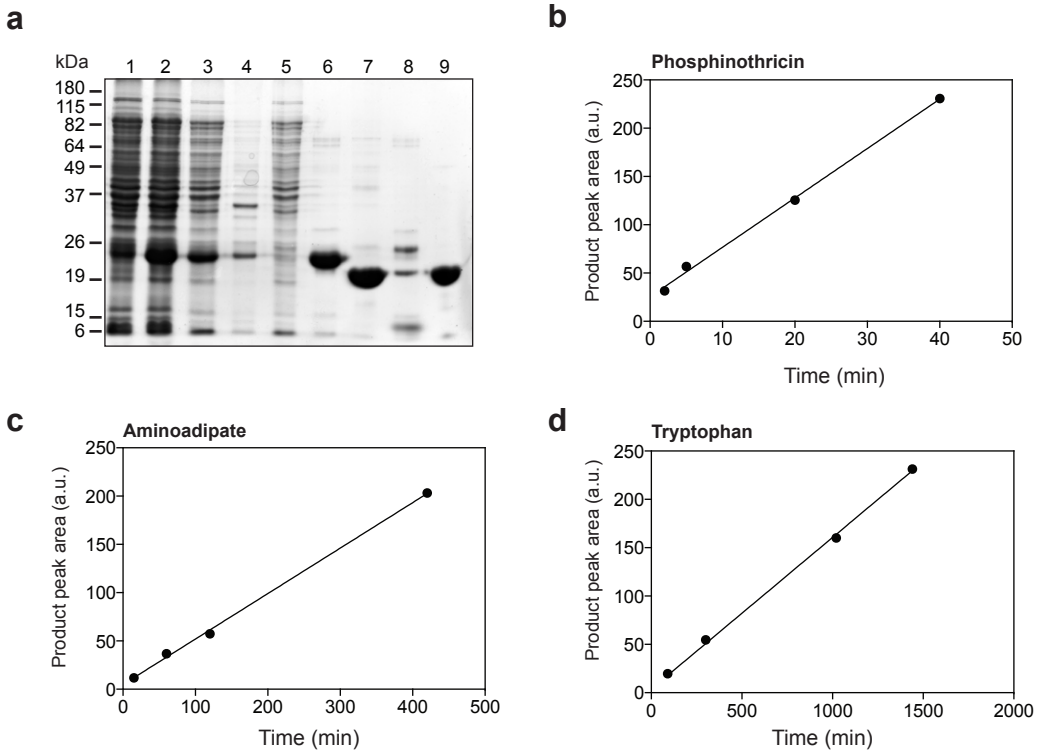

Supplementary Figure 6 | Purification and time-dependent activities of recombinant BAR from *E.coli.* a, BAR expression and purification was monitored by SDS-PAGE. The 6xHis-BAR protein fusion was isolated from the *E. coli* lysate (lane 1, uninduced cells; lane 2, induced cells; lane 3, soluble proteins; lane 4, insoluble proteins) by metal affinity chromatography (Ni^{2+}-charged HisTrap (GE Healthcare)); lane 5, flow-through; lane 6, 6xHis-BAR elution). Partially purified 6xHis-BAR protein fusion was then treated with 6xHis-TEV protease[37] and passed through the HisTrap to remove the His-tag (lane 7, flow-through; lane 8, elution of 6xHis-TEV and uncut 6xHis-BAR) and further purified by gel exclusion chromatography (lane 9). Time-dependent activities of purified 6xHis-BAR were determined at substrate concentration of 500 µM for phosphinothricin (**b**) and 1000 µM for aminoadipate (**c**) and tryptophan (**d**). a.u., arbitrary unit.

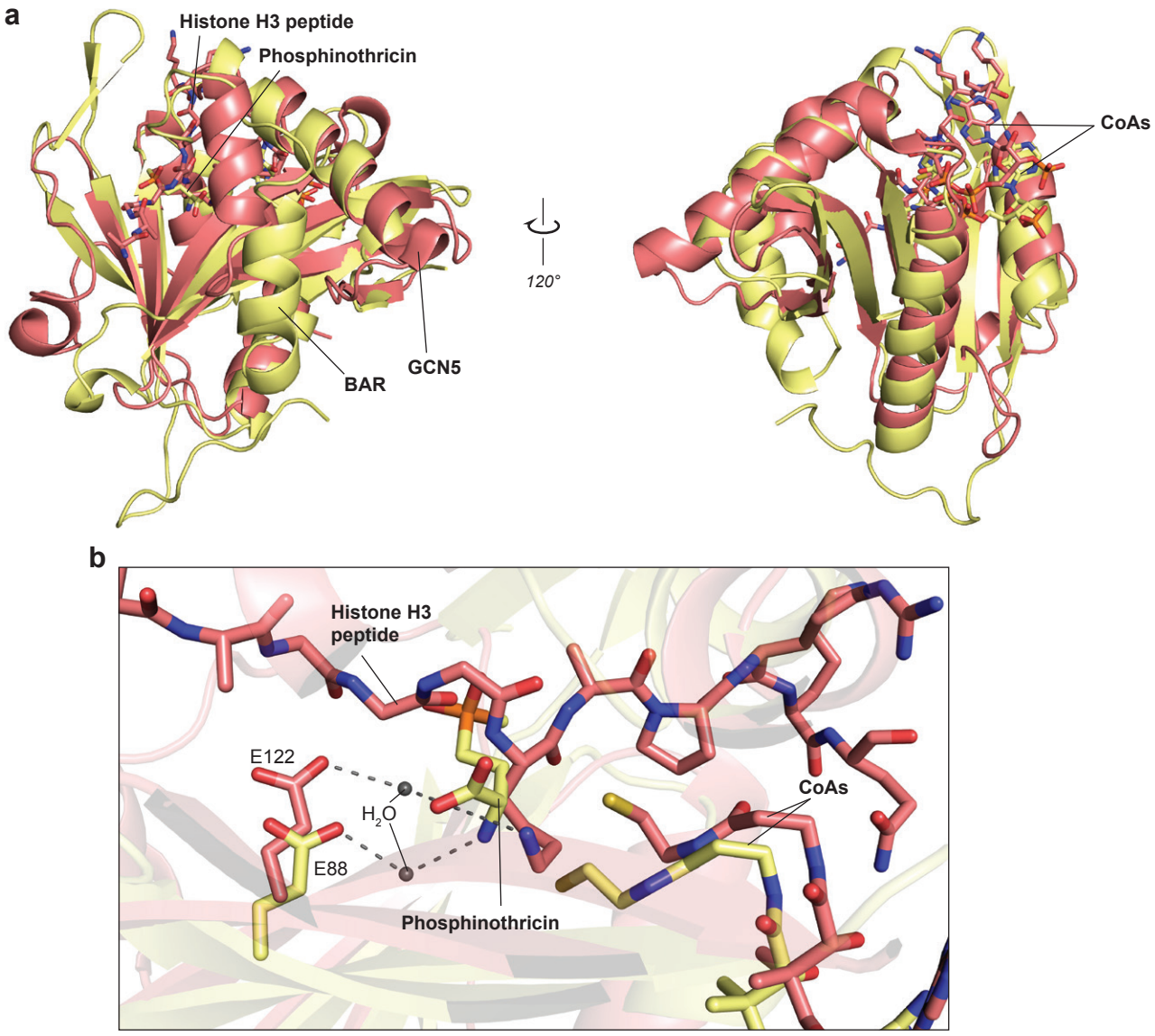

Supplementary Figure 7 | Structural alignment of BAR/CoA/phosphinothricin ternary complex (yellow) and *Tetrahymena* GCN5 bound to CoA and histone H3 peptide (red, PBD ID: 1QSN). a, Diagram showing two views of the alignment perfomed using the SSM structural alignment function under Coot[41]. **b**, Close-up view of the active site.

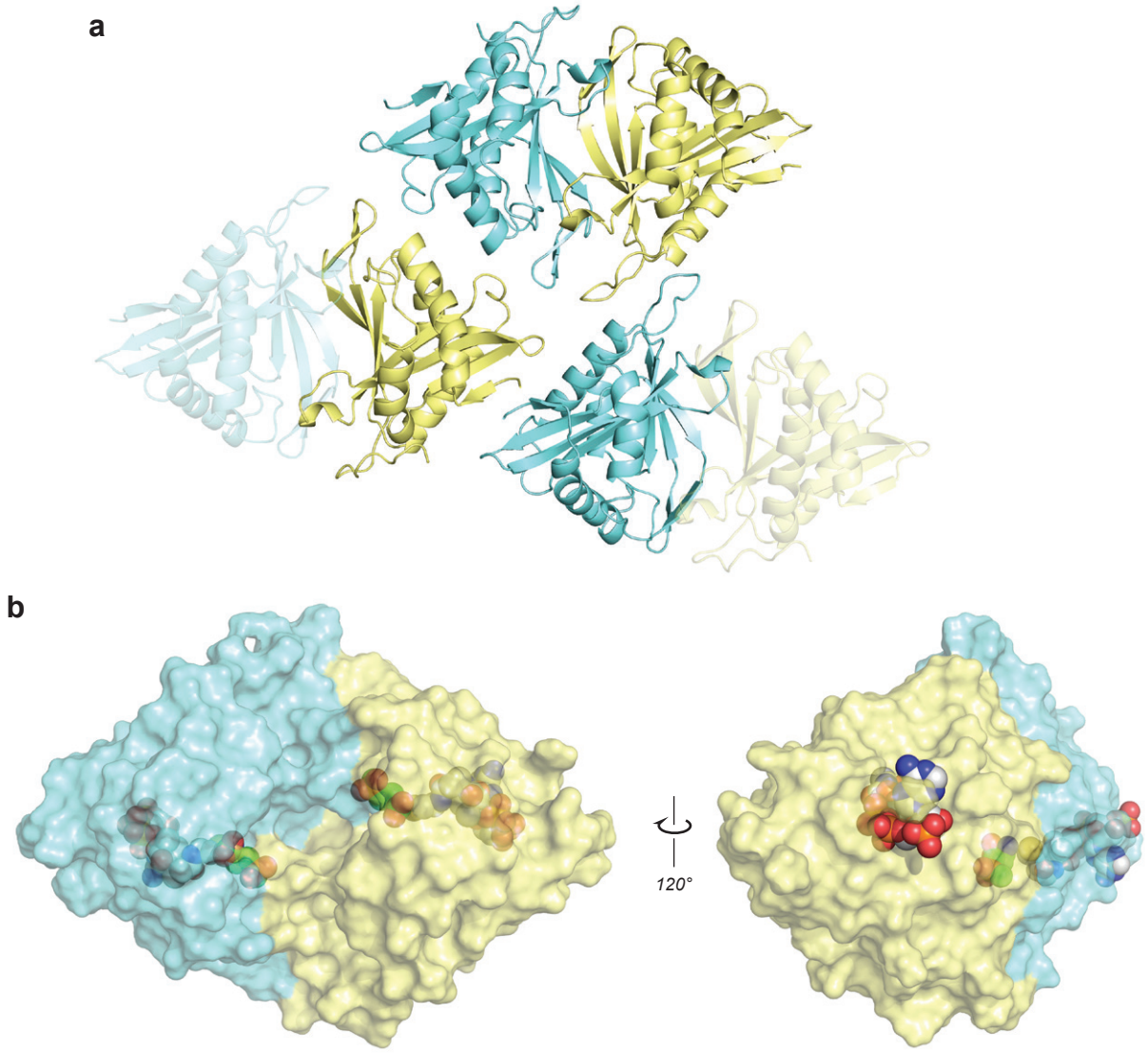

Supplementary Figure 8 | BAR crystallizes as homodimer with two active sites symmetrically distributed around the dimer interface. a, Each asymmetric unit (ASU) is constituted of one homodimer and two monomers that form homodimer with chains from neighboring cells (shown as transparent chains). **b**, Surface representation of BAR revealing a large open cavity at the dimer interface.

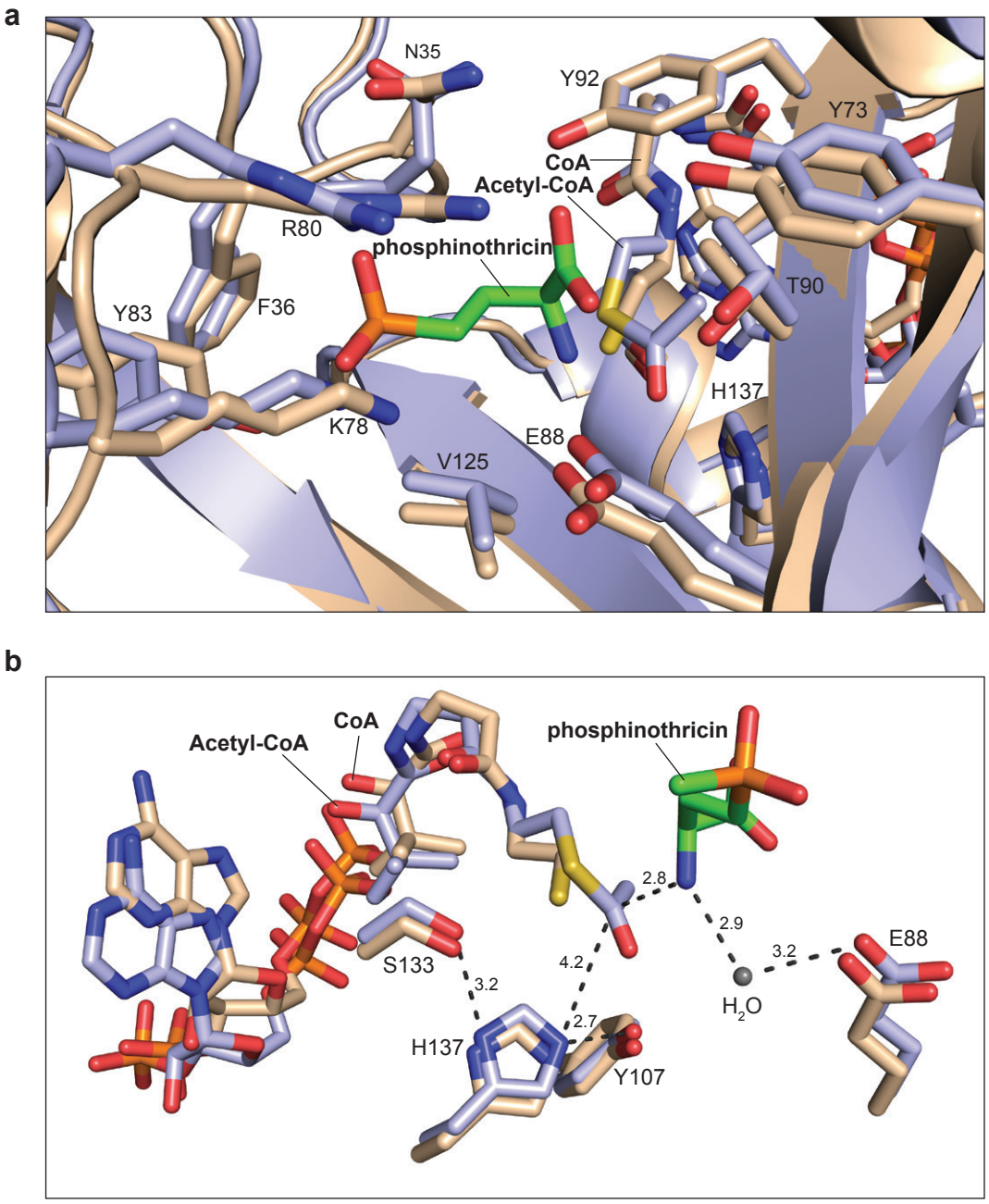

Supplementary Figure 9 | Structural alignment of the BAR/acetyl-CoA holocomplex (purple) with the BAR/CoA/phosphinothricin ternary complex (brown). a, Close-up of view of the active site of BAR. **b**, Diagram showing the residues involved in catalysis. Distances are shown in Angstroms.

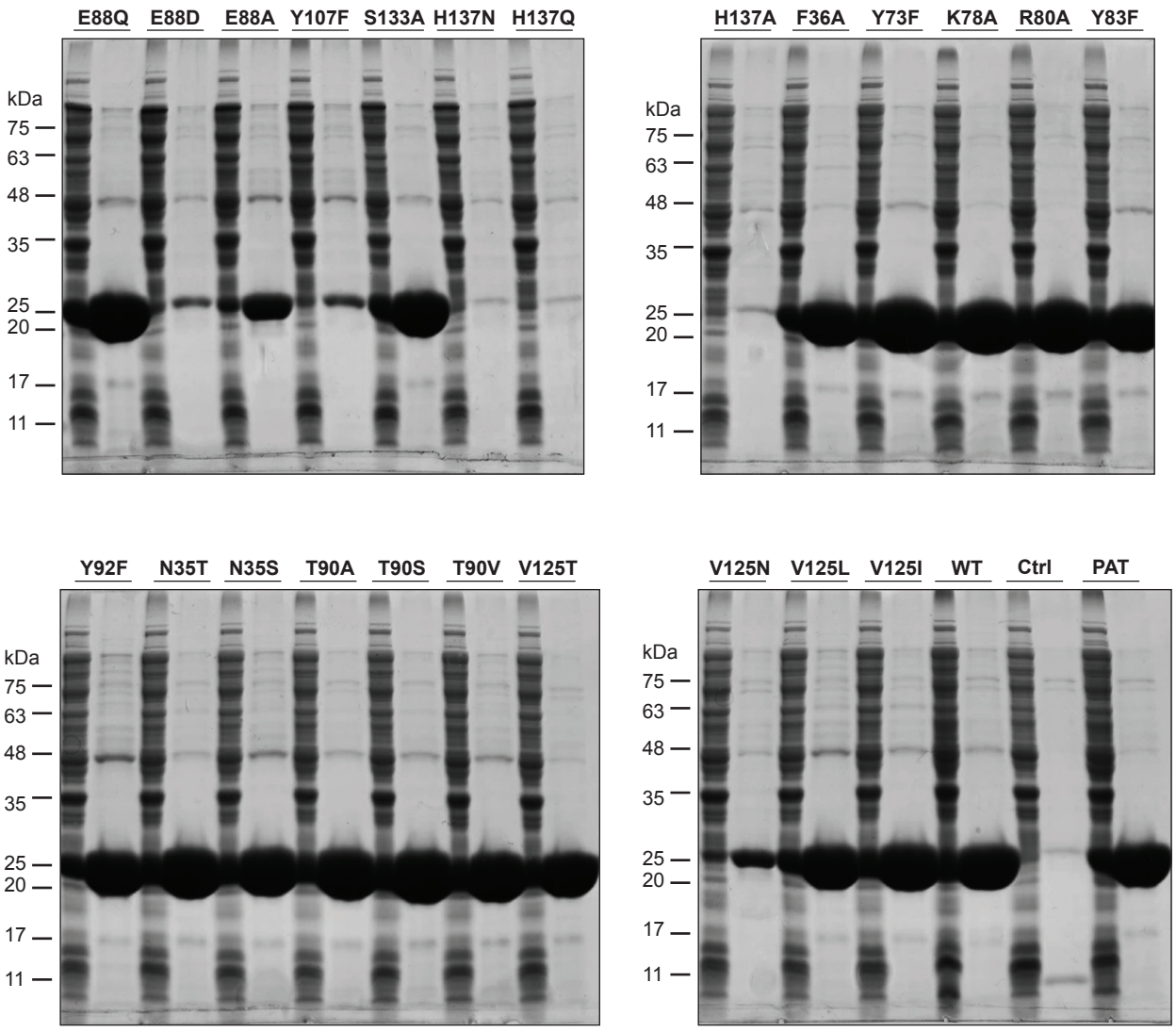

Supplementary Figure 10 | Expression and purification of 23 recombinant mutant versions of BAR and wild-type PAT from *E.coli*. Left SDS-PAGE lane, soluble fraction of *E.coli* lysate; right lane, purified protein; Ctrl, empty vector.

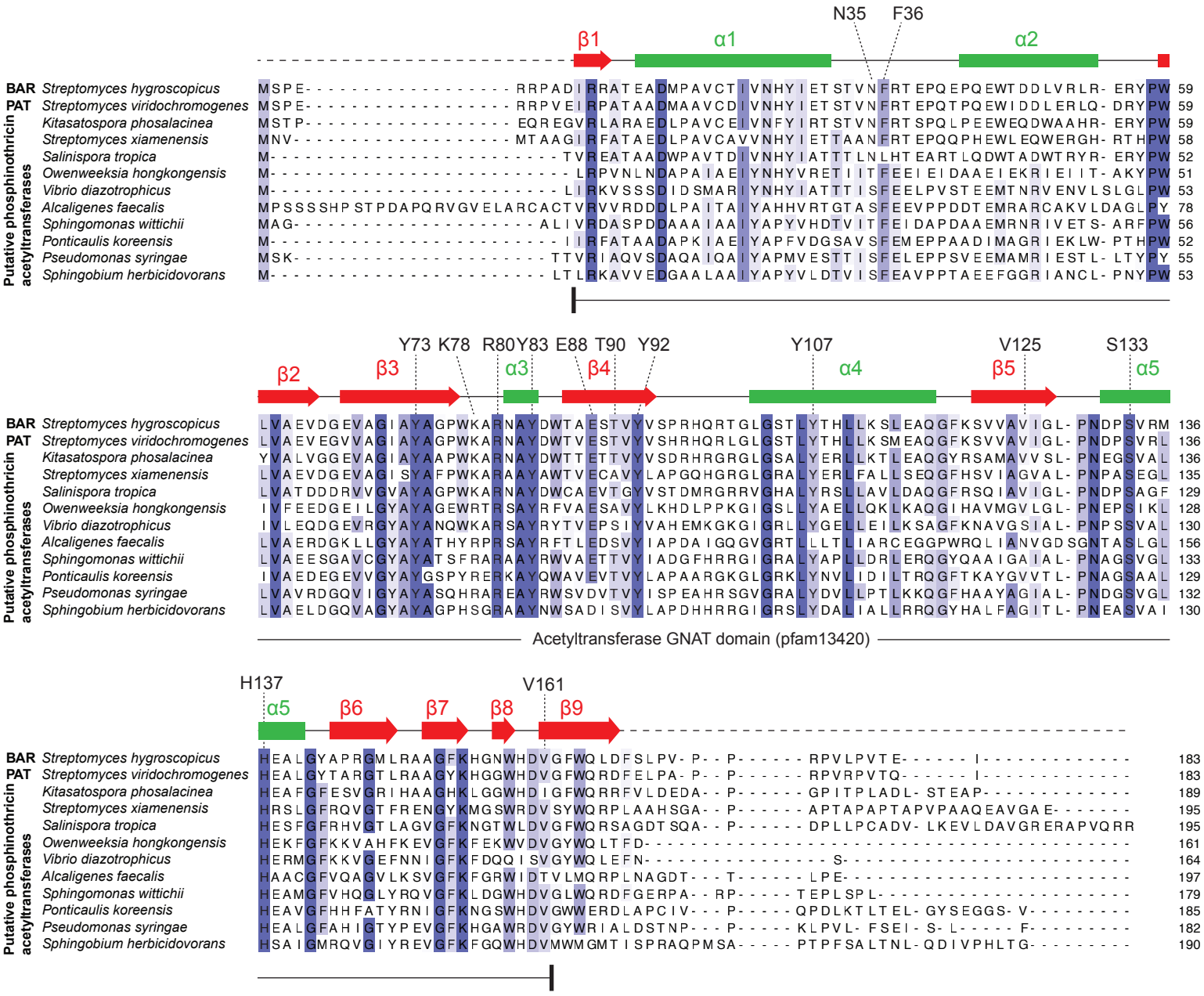

Supplementary Figure 11 | Protein sequence alignement of BAR from *Streptomyces hygroscopicus*, PAT from *Streptomyces viridochromogenes* and closely related homologues from other species. Active site residues as displayed in Fig. 4b are labelled. The alignment was performed using Jalview V2 (T-Coffee, default settings[53]). Secondary structure of BAR as labelled in Fig. 4a is shown. The acetyltransferase GNAT domain (pfam13420) is displayed. Protein sequences related to BAR from *Streptomyces hygroscopicus* were retrieved from GenBank at the NCBI website using protein BLAST search (http://blast.ncbi.nlm.nih.gov/Blast.cgi). Protein sequence accessions (GenBank): *Streptomyces hygroscopicus*: CAA29262; *Streptomyces viridochromogenes*, WP_003988626; *Kitasatospora phosalacinea*, WP_033213694; *Streptomyces xiamenensis*, AKG45686; *Salinispora tropica*, WP_028566484; *Owenweeksia hongkongensis*, WP_014202881; *Vibrio diazotrophicus*, WP_042485812; *Alcaligenes faecalis*, CAA00175; *Sphingomonas wittichii*, WP_037526498; *Ponticaulis koreensis*, WP_022694195; *Pseudomonas syringae*, WP_032656505; *Sphingobium herbicidovorans*, WP_037462269.

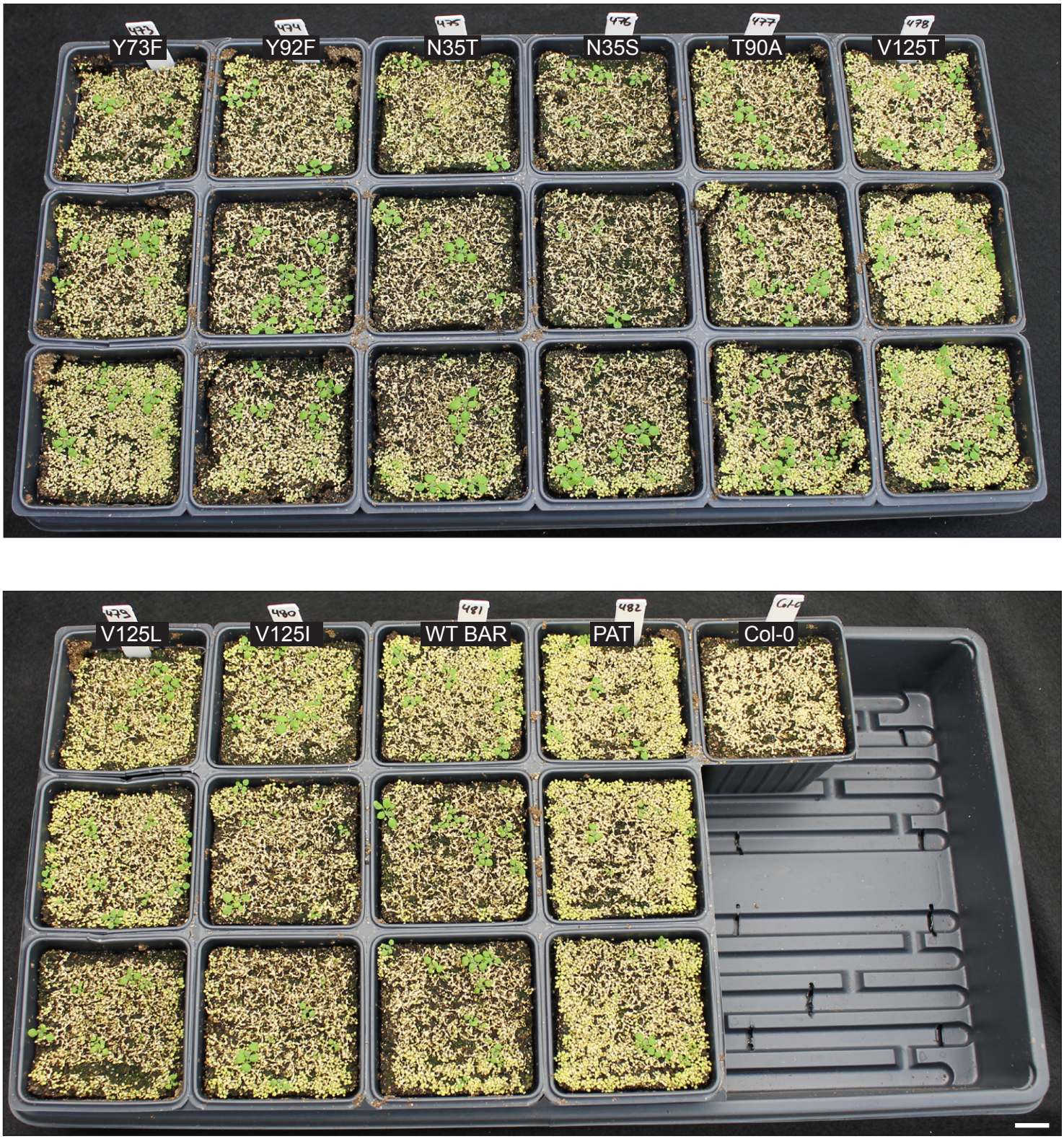

Supplementary Figure 12 | Selection of T1 transgenic Arabidopsis transformed with BAR variants. Photographs of Arabidopsis T1 lines transformed with wild-type BAR from *Streptomyces hygroscopicus* (WT BAR), PAT from *Streptomyces viridochromogenes* and selected BAR mutants taken 10 days after Finale® application. Scale bar = 1 cm

Supplementary Figure 13 | Resistance to phosphinothricin of T2 transgenic Arabidopsis transformed with BAR variants. 17-day old transgenic T2 plants were sprayed with Finale® and further grown for 8 days. b, Photographs were taken before and after Finale® application. Scale bar = 1 cm

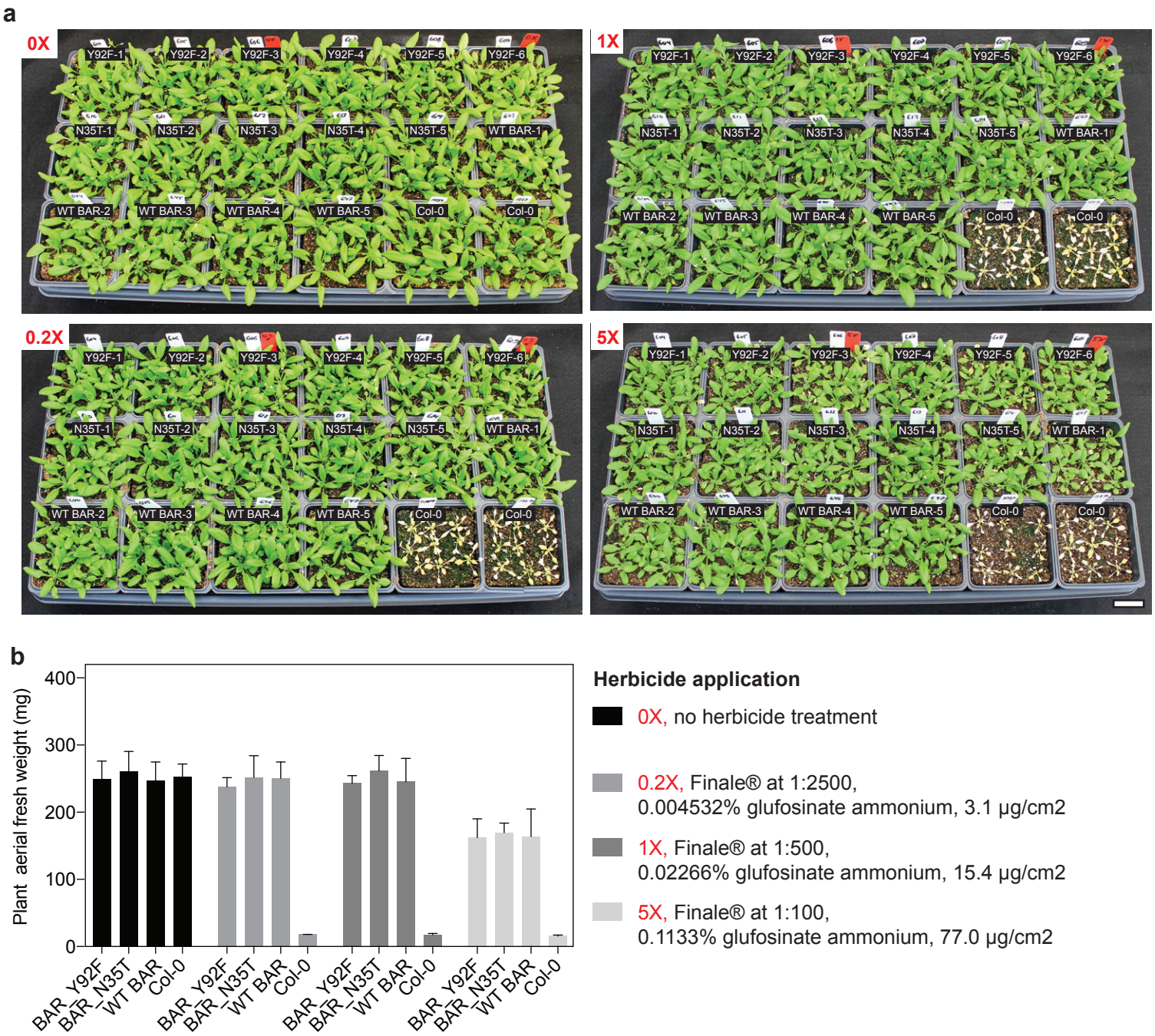

Supplementary Figure 14 | Resistance to phosphinothricin of transgenic Arabidopsis transformed with BAR variants Y92F, N35T and WT BAR. a, Seventeen-days old transgenic T2 plants were sprayed with 3 different concentrations of Finale® and further grown for 8 days. Photographs were taken 8 days after Finale® application. Scale bar = 1 cm. **b**, Average fresh weight were measured for each population 8 days after Finale® application. Error bars, mean of plant aerial fresh weight ± s.d. (n = 6 (Y92F), 5 (N35T), 5 (WT BAR), 2 (Col-0) biological replicates from individual populations). The weight of 7-9 plants were measured and average for each individual population.

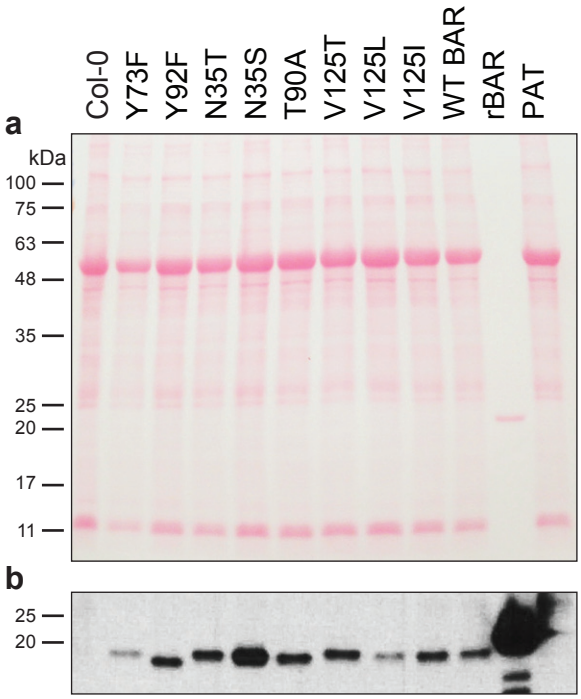

Supplementary Figure 15 | Protein levels of BAR variants in Arabidopsis. **a**, Total proteins were extracted from T2 plants, separated by SDS-PAGE, transferred to nitrocellulose membrane and stained by Ponceau S. For each protein extraction, equal amounts of aerial tissues from 5-6 T2 populations grown from seeds from independent T1 plants were pooled. **b**, Detection of BAR by anti-BAR immunoblotting of the membrane shown in panel (**a**). rBAR, recombinant BAR from *E.coli*.

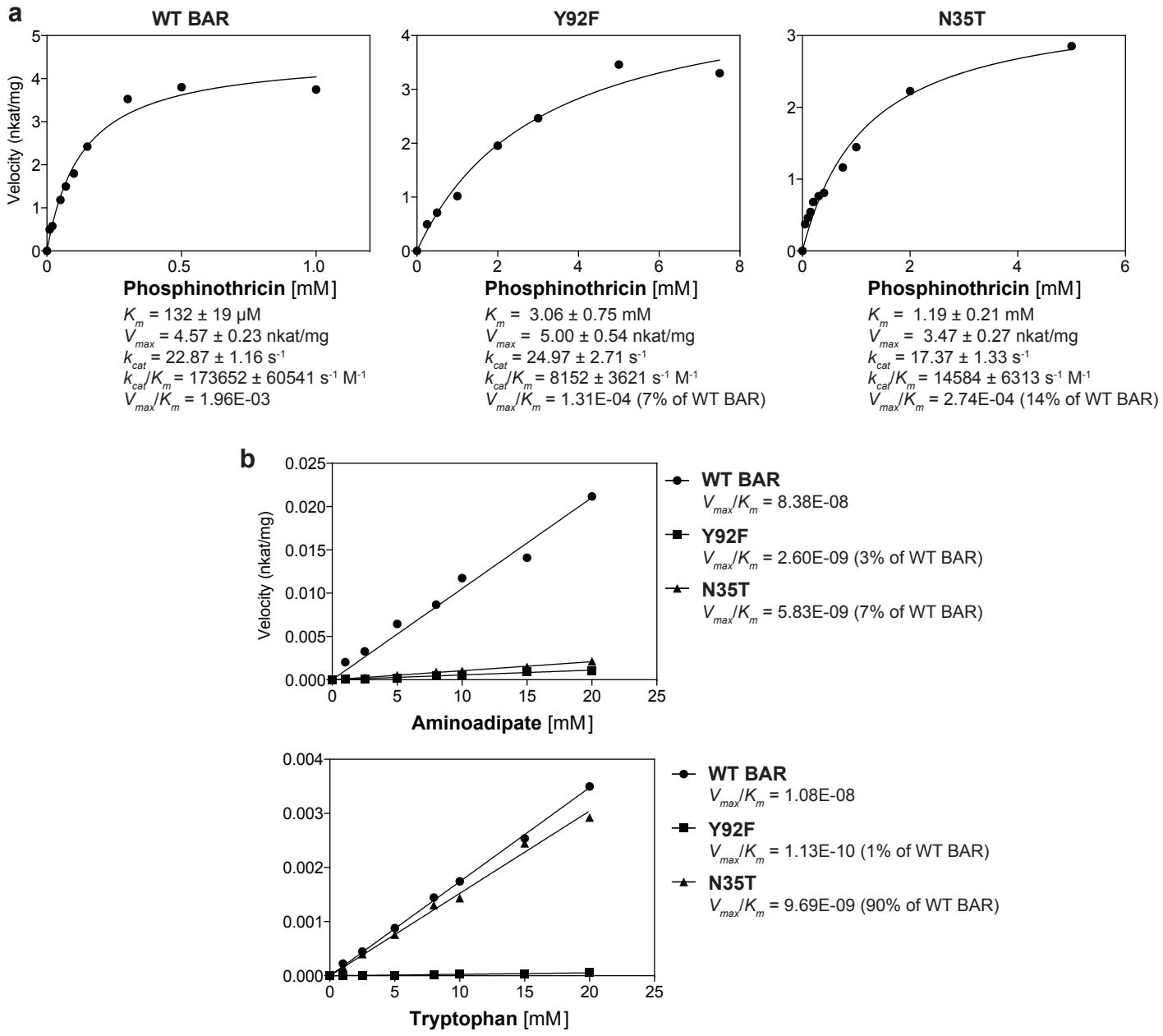

Supplementary Figure 16 | *In vitro* enzyme kinetic assays of wild-type BAR (WT BAR, as shown in Fig. 3) and BAR variants Y92F and N35T against native (a) and non-native substrates (b). Calculated K_m, V_{max}, k_{cat}, k_{cat}/K_m and V_{max}/K_m values for phosphinothricin are indicated, as well V_{max}/K_m values for aminoadipate and tryptophan (estimated from Lineweaver-Burk plots). Note that aminoadipate and tryptophan reached solubility limit before reaching saturation concentration for WT BAR, Y92F and N35T.

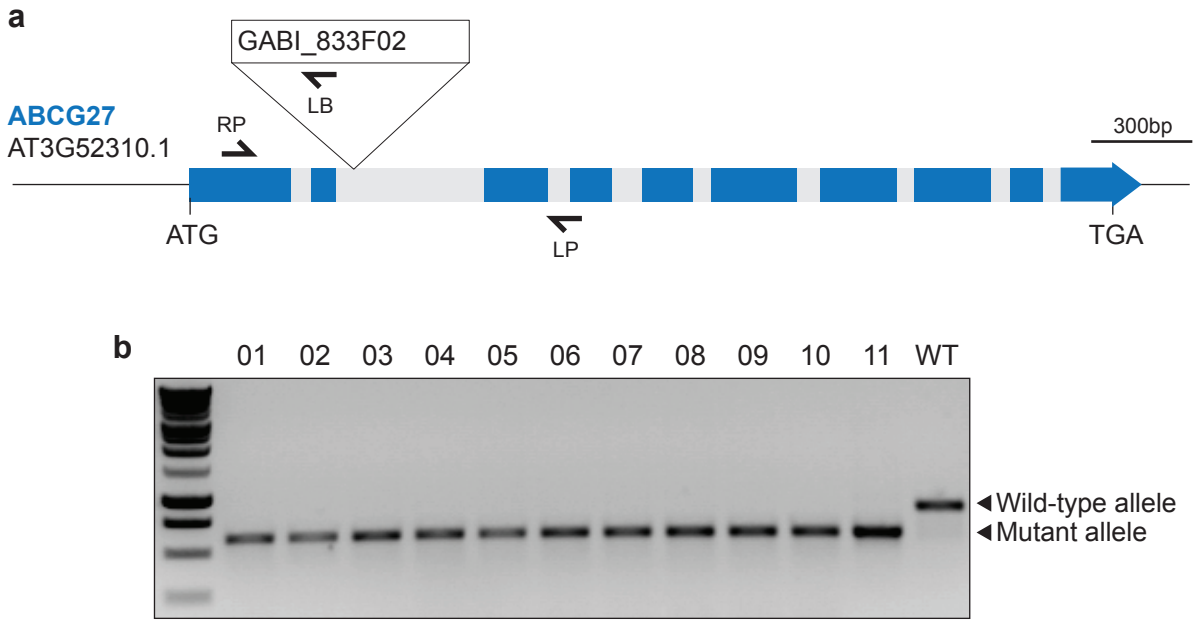

Supplementary Figure 17 | Genotyping of GABI_833F02. a, Gene structure of Arabidopsis ABCG27 (AT3G52310.1). Exons and introns are depicted in blue and gre, respectively. The T-DNA insertion site and genotyping primers are indicated. ATG and TGA depict start and stop codons. **b**, Genotyping by PCR of 11 homozygous mutant plants of GABI_833F02 (PCRs were performed with the 3 primers shown in (**a**) in single reactions). WT, Wild-type Columbia-0 control.